

See discussions, stats, and author profiles for this publication at: <https://www.researchgate.net/publication/12727137>

# Ripple depth and density resolution of rippled noise

Article in *The Journal of the Acoustical Society of America* · December 1999

DOI: 10.1121/1.428105 · Source: PubMed

---

CITATIONS

37

---

READS

40

4 authors, including:



Vladimir Vladimirovich Popov

Severtsov Institute of Ecology and Evolution

104 PUBLICATIONS 1,443 CITATIONS

SEE PROFILE

# Ripple depth and density resolution of rippled noise

A. Ya. Supin, V. V. Popov, O. N. Milekhina, and M. B. Tarakanov

*Institute of Ecology and Evolution, Russian Academy of Sciences, 33 Leninsky Prosp., 117071 Moscow, Russia*

(Received 13 August 1998; accepted for publication 22 July 1999)

Depth resolution of spectral ripples was measured in normal humans using a phase-reversal test. The principle of the test was to find the lowest ripple depth at which an interchange of peak and trough position (the phase reversal) in the rippled spectrum is detectable. Using this test, ripple-depth thresholds were measured as a function of ripple density of octave-band rippled noise at center frequencies from 0.5 to 8 kHz. The ripple-depth threshold in the power domain was around 0.2 at low ripple densities of 4–5 relative units (center-frequency-to-ripple-spacing ratio) or 3–3.5 ripples/oct. The threshold increased with the ripple density increase. It reached the highest possible level of 1.0 at ripple density from 7.5 relative units at 0.5 kHz center frequency to 14.3 relative units at 8 kHz (5.2 to 10.0 ripple/oct, respectively). The interrelation between the ripple depth threshold and ripple density can be satisfactorily described by transfer of the signal by frequency-tuned auditory filters. © 1999 Acoustical Society of America. [S0001-4966(99)02011-1]

PACS numbers: 43.66.Fe, 43.66.Jh [RVS]

## INTRODUCTION

Spectral shape resolution is of obvious importance for discriminating complex acoustic stimuli. It has been a subject of many psychophysical studies with the use of various signal types as complex sounds. A productive approach to study spectral shape discrimination is ‘profile analysis’ when a signal is composed of a number of sinusoids; the adjustment of sinusoid amplitudes results in various spectral profiles (e.g., Green, 1983, 1988, 1992; Green *et al.*, 1984, 1987). Using this approach, various alterations of spectral shape were tested, in particular, increments to a single component, step functions, and sinusoidal ripples. Those studies used rather wide frequency spacing between adjacent components which made them addressing to different critical bands. Thus, the studies were addressed mainly to the question of how the auditory system compares intensity information in different frequency channels (Durlach *et al.*, 1986).

Another way was to use rippled spectra which imitate coarse or fine spectrum patterns depending on the ripple density. Many studies using rippled noise were directed to investigate pitch perception mechanisms (Yost *et al.*, 1977, 1996; Yost and Hill, 1979; Bilsen and Wieman, 1980; Yost, 1982; Patterson *et al.*, 1996). However, rippled noise can be considered as a model for complex sounds irrespective of the involved mechanisms. The resolvable ripple density (spacing) can be used as a measure of the spectrum pattern resolution (Supin *et al.*, 1994, 1997, 1998).

In those studies, major attention was paid for discrimination of spectral patterns with various ripple densities. For a better knowledge of spectral shape analysis, discrimination of both ripple density and ripple depth should be studied. For this purpose, a reliable model could be rippled spectra which vary both in ripple density and in ripple depth. In previous studies (Popov and Supin, 1984; Supin *et al.*, 1994) we have made preliminary measurements of ripple-depth thresholds

as a function of ripple density. These measurements were made using only wideband rippled noise; thus, a question remained whether the ripple-depth threshold versus ripple density dependence is one and the same in any part of the frequency range of hearing.

Therefore, in the present study we investigated the ripple-depth threshold dependence versus ripple density using narrow-band rippled noises of different center frequencies. In order to make the results comparable with those obtained earlier, we used the same experimental paradigm as in our preceding studies (Supin *et al.*, 1994, 1997). Namely, to find the ripple depth discrimination limit, we used the phase reversal test. Its principle is depicted in Fig. 1. Rippled noise of a certain ripple depth and density is presented to a listener. At a certain instant, it is replaced by a noise of the same intensity, bandwidth, ripple depth, and density but with the opposite positions of spectral peaks and troughs at the frequency scale, i.e., ripple phase reversal occurs. This spectra pair is shown in Fig. 1 by open and filled areas. The listener can only detect this switch if he discriminates the rippled spectrum pattern. If the spectrum pattern is not resolvable since the ripple depth is too small, or the ripples are spaced too densely, or both, the switch cannot be detected because the noise before and after the switch is the same in all respects except for the peak and trough positions. Thus, the threshold ripple depth at a certain ripple density can be found. Immediate replacing of one spectral pattern by another makes the test addressing to sensory abilities without involving short-term memory, contrary to successive presentation of two compared stimuli with an interval between them. This approach is quite similar to one widely used to measure visual acuity: in both cases the phase reversal of a test grid is used to find the contrast threshold as a function of grid density.

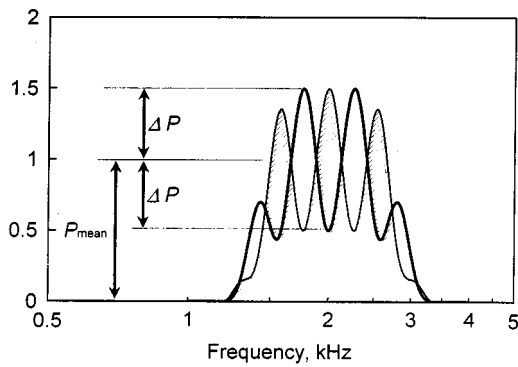


FIG. 1. Examples of rippled spectra with a center frequency of 2 kHz. Relative ripple density 4, ripple density 0.5. Filled and open areas—rippled spectra which replace one another at the phase-reversal test. Parameters  $P_{\text{mean}}$  and  $\Delta P$  are indicated by arrows. Ripple spacing looks constant at the logarithmic frequency scale, i.e., ripple density is frequency proportional.

## I. MATERIAL AND METHODS

### A. Subjects

Five subjects (laboratory staff) were used. They were 25 to 38 years old and had no signs of hearing loss. All had praxis in psychoacoustic experiments. The experiments were performed in accordance with the guidelines of the Declaration of Helsinki.

### B. Stimulus parameters

Rippled noise stimuli used in this study were of octave equivalent rectangular bandwidth (ERB). Their power spectra were enveloped by a function which was flat within  $\pm 0.25$  octave from the center frequency and bounded by two quarter-octave ramps which were cosine functions of frequency logarithm (Fig. 1). The shallow-ramped spectrum shape was chosen since sharp spectral edges result in edge effects increasing ripple resolution (Supin *et al.*, 1998). Within this envelope, spectra had ripples which were described by a cosine function (in the power domain) of frequency logarithm (frequency-proportional spaced).

To characterize a ripple pattern, two main parameters were used: ripple density and depth. The ripple density was defined as a ratio of the center frequency to ripple spacing (relative density):

$$D_{\text{rel}} = F_0 / \delta F, \quad (1)$$

where  $D_{\text{rel}}$  (relative units) is the density,  $F_0$  (kHz) is the center frequency of a ripple cycle, and  $\delta F$  (kHz) is the ripple spacing. Since ripples were frequency proportional, the density  $D_{\text{rel}}$  was constant across the bandwidth. In this case, the ripple density can also be characterized as a number of ripples per octave ( $D_{\text{oct}}$ , cycles/oct). There is a constant ratio between these two metrics:  $D_{\text{oct}} \approx D_{\text{rel}} \ln 2 \approx 0.7 D_{\text{rel}}$ . Below we use both metrics to characterize the ripple density: the relative and octave density.

Ripple depth was defined as a relative deviation of peaks and troughs from the mean level:

$$m = \Delta P / P_{\text{mean}} = (P_{\text{max}} - P_{\text{min}}) / (P_{\text{max}} + P_{\text{min}}), \quad (2)$$

where  $m$  is the ripple depth,  $\Delta P$  is the deviation from the mean power density  $P_{\text{mean}}$ , and  $P_{\text{max}}$  and  $P_{\text{min}}$  are the power densities at ripple peaks and troughs, respectively. With these definitions, Fig. 1 exemplifies spectra with a center frequency of 2 kHz, ripple density of  $D_{\text{rel}} = 4$  ( $D_{\text{oct}} = 2.8$ ), and ripple depth of 0.5. Note that the ripples seem equally spaced being presented at the logarithmic frequency scale.

The following stimulus parameters were used. Center frequencies were 0.5, 1, 2, 4, and 8 kHz. Ripple density  $D_{\text{rel}}$  varied by steps as follows: 4, 5, 6, 7, 8, 10, 12, 14, 16, 20, 24, 28, and 32 relative units (which corresponds to  $D_{\text{oct}}$  of 2.8 to 22.4 cycles/oct); densities lower than  $D_{\text{rel}} = 4$  ( $D_{\text{oct}} = 2.8$ ) were not tested because of an insufficient number of ripples (less than 3) within the noise bandwidth. Ripple depth defined according to Eq. (2) varied in steps: 0.05, 0.1, 0.15, 0.2, 0.3, 0.5, 0.7, and 1.

### C. Signal generation

The signals were digitally generated at sampling rates of 10, 14, 20, 28, or 40 kHz, keeping the sampling rate at least four times higher than the center frequency of the signal but not lower than 10 kHz and not higher than 40 kHz. The generation program simulated steps as follows. A wideband signal (random digital sequence with the sampling rate, uniformly distributed between  $\pm 1$ ) was filtered by one of the two digital filters. Frequency responses of the filters used are of the type shown in Fig. 1. The filters determined both the noise passband and ripple pattern (ripple density and depth). To perform filtering, a specified filter form was inversely Fourier transformed to obtain the temporal transfer function. Then the wideband signal (random digital sequence) was convoluted with the transfer function; the result was a filtered rippled noise.

To generate a signal with ripple phase-reversals, two filters were used which had equal passbands, levels, ripple densities, and depths but opposite ripple peak-trough positions (see Fig. 1). Phase reversals were performed by switching the wideband signal from one filter input to another; filter outputs were summed. If a noise burst without phase reversals was generated, the same procedure was used but both filters were identical.

Note that phase-reversal switches were made at the filter inputs, not outputs. Otherwise, clicks at phase reversals could arise. With phase reversals at the filter inputs, neither signal discontinuity nor transient spectrum splatter appeared at the filter outputs. Since both of the filters had equal rise-fall times (which was a direct consequence of their equal bandwidths), the signal level decay at one filter output was compensated by the signal level rise at another filter output, thus the switch did not result in any transient level shift exceeding fluctuations intrinsic in narrow-band noise. The generation procedure were described in more detail (Supin *et al.*, 1998).

Each noise burst (either with or without phase reversals) lasted 2 s. Phase reversals, if present, occurred every 333 ms, i.e., a burst with phase reversals contained three cycles of switching from one filter to another and back. These param-

eters were used since the phase-reversal rates higher than 1.5/s led to decreased ripple resolution (Supin *et al.*, 1997), and since the listeners reported that they needed at least a few seconds to listen to the signal and to decide whether the stimulus did or did not contain some alternations.

Pregenerated noise bursts were stored in computer memory. During experiments, they were played through a 14-bit D/A converter, amplified, attenuated, and presented diotically over TDS-7 earphones with the frequency response irregularity of no more than 10 dB within the range of 0.1–6 kHz and no more than 18 dB within the range of 0.1–16 kHz. A listener could choose a level which he considered to be the most comfortable and providing the easiest stimulus discrimination. A chosen level was constant for a given listener across all stimulation conditions. These levels were within a range of 70–80 dB SPL.

## D. Procedure

A three-interval 2AFC procedure was used. Each trial consisted of three noise bursts, each of 2-s duration with 0.5-s intervals between them. Two trial types alternated randomly: either the first and third bursts contained phase reversals and the second did not contain them, or the second burst contained the phase reversals and the first and third did not. The listener knew that the first and third bursts were identical and different from the second one. The listener's task was to detect any modifications in the noise and to report whether they appeared in the first and third bursts or in the second one. The listener was informed of whether the response was true or false. Thus, the procedure was two-alternative and differed from a standard one in only the additional third signal which always duplicated the first one. This modification was used since the listeners reported that they were more confident to make a decision in the three-interval procedure rather than in the standard two-interval one: they could make a decision by comparing the first and second bursts and then verify it by comparing the second and third ones.

During a measurement run, ripple depth varied adaptively (one-up, two-down procedure) by steps indicated above (Sec. 1B). This procedure causes stimuli to vary around a value providing 70.1% true responses which is close to the 75% threshold criterion (Levitt, 1971). Contrary to the standard Levitt's procedure, we used the adaptive stimulus presentation only to provide most of the signals to be just above and just below the threshold level. The threshold was calculated as in a constant-stimuli procedure, i.e., percentage of true responses was counted for presented values, and a ripple-depth value corresponding to 75% of true responses was found by interpolation between the nearest values. This threshold calculation provided better accuracy because of the use of the entire body of near-threshold data instead of a lesser number of extremes. On the other hand, because of the adaptive stimuli presentation, a majority of stimuli had one of two values (just above or just below the threshold) which were used for interpolation. This minimized the overall number of trials. Runs lasted until stimuli providing true response probability just above and just below the 75% level were presented 20 times each. It required 50 to

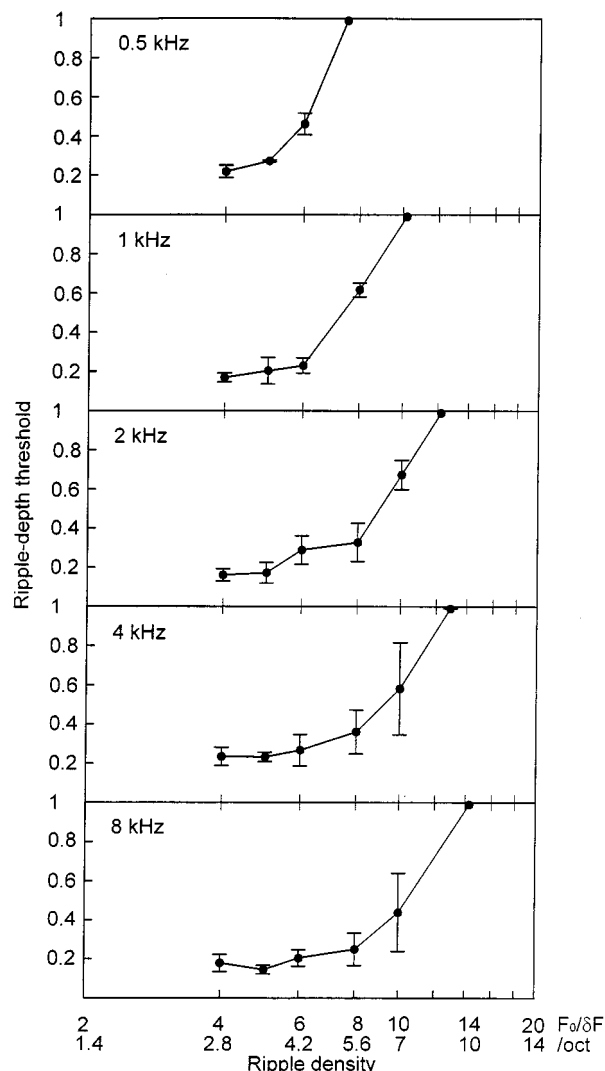


FIG. 2. Ripple depth threshold versus ripple density dependence for center frequencies from 0.5 to 8 kHz, as indicated. Interindividual averaging of data for five listeners (mean  $\pm$  s.d.). Ripple density is indicated in two measures: upper scale—relative density ( $F_0/\Delta F$ ), lower scale—octave density (number of ripples per octave).

70, sometimes up to 100 trials. Except for a few cases, two runs were used to obtain a threshold estimate.

The measurement runs were repeated at various ripple densities to obtain ripple-depth thresholds as a function of ripple density at a certain center frequency. The last point of the function was obtained by keeping the modulation depth at a constant level of 1.0 and varying ripple density. In these runs, the procedure was the same as described above, except that the ripple density was used as the varying parameter. Then all the measurement sets were repeated at different center frequencies.

## II. RESULTS

The results of measurement are presented in Fig. 2 showing ripple-depth thresholds as functions of ripple density at various center frequencies, from 0.5 to 8 kHz. All the curves were characterized with low ripple-depth thresholds at low ripple densities and increased thresholds at higher

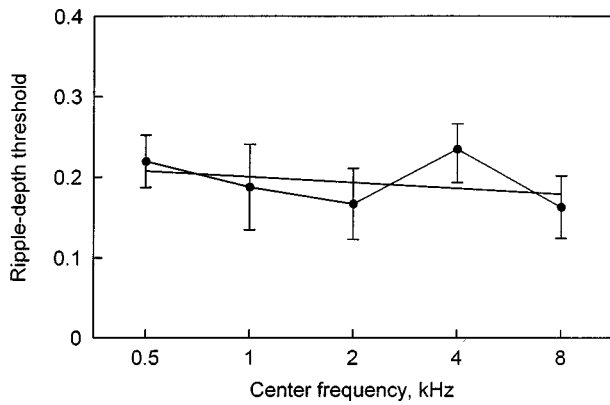


FIG. 3. Minimal ripple depth threshold versus center frequency dependence. Averaged data for five listeners at relative ripple densities of 4 and 5 (except a frequency of 0.5 kHz: data for ripple density 4 only) (mean  $\pm$  s.d.). The trend is shown by a straight line.

ripple densities. At low ripple densities ( $D_{\text{rel}}$  of 4 to 5,  $D_{\text{oct}}$  of 2.8 to 3.5), ripple-depth thresholds were from 0.15 to 0.27 at all center frequencies. Although some variation from one center frequency to another was observed, the trend was very little and insignificant (Fig. 3). So, it seemed reasonable to average the data across all the center frequencies to obtain a mean value of modulation depth threshold. This value was estimated as  $0.19 \pm 0.05$  s.d.

At ripple densities higher than  $D_{\text{rel}}$  of 6 to 8 ( $D_{\text{oct}}$  of 4.2 to 5.6), ripple-depth thresholds rose steeply and reached the maximal value of 1.0 at ripple densities from  $D_{\text{rel}}=7.5$  ( $D_{\text{oct}}=5.2$ ) at 0.5-kHz center frequency to  $D_{\text{rel}}=14.3$  ( $D_{\text{oct}}=10.0$ ) at 8 kHz. These end points of the curves were found by varying the ripple density at a constant depth of 1.0; they represent ripple-density resolution limits at the used center frequencies.

### III. DISCUSSION

#### A. Ripple-depth threshold

The ripple-depth threshold obtained herein (0.19) is close to the value (0.2) reported for wideband rippled noise (Supin *et al.*, 1994). In profile analysis experiments with the use of wideband signals composed of a number of sinusoids, a similar threshold for spectral contrast was found at low ripple densities (Green, 1983, 1987, 1988). Note, this value is for spectrum presentation in the power domain but not in the magnitude domain where the same value is around 0.1. Thus, the data presented herein show that the ripple-depth threshold does not depend significantly on frequency within a rather wide frequency range.

#### B. Interrelation between ripple depth and density

With increasing ripple density, ripple-depth threshold increases until it reaches the highest level of 1.0 at a ripple-density resolution limit. A simple model based on interaction between rippled spectra and frequency-tuned auditory filters may be proposed to explain this interrelation. It should be noted that both frequency-tuning processing [frequency-dependent masking studies by Houtgast (1974, 1977), Pick *et al.* (1977) and Pick (1980); ripple-density resolution stud-

ies by Wilson and Evans (1971) and Supin *et al.* (1994)] and temporal processing [pitch discrimination studies by Yost *et al.* (1996) and Patterson *et al.* (1996)] were suggested as mechanisms of rippled spectrum discrimination. Independent of the involved mechanisms, signal processing can be described in either temporal or frequency-spectrum domain. We use the spectral description as convenient for our purposes.

For definiteness sake, define the filter shape by a rounded exponential (roex) function (Patterson *et al.*, 1982):

$$W(g) = (1 + pg)\exp(-pg), \quad (3)$$

where  $W$  is the output power,  $g$  is the relative deviation from the filter center frequency, and  $p$  is a parameter determining the filter tuning. For this filter form, the relative equivalent rectangular bandwidth  $E$  is equal to  $4/p$ , thus

$$W(g) = (1 + 4g/E)\exp(-4g/E). \quad (4)$$

Rippled power spectra of opposite peak-trough positions are defined as

$$P(g) = 1 \pm m \cos 2\pi Dg, \quad (5)$$

where  $D$  is the relative ripple density and  $m$  is the ripple depth. The power  $P_{\text{peak}}$  transmitted by the filter when a ripple peak is centered on the filter (spectrum  $1 + m \cos 2\pi Dg$ ) is

$$P_{\text{peak}} = 2 \int_0^\infty W(g)P(g) dg = E[1 + m/(1 + \pi^2 D^2 E^2/4)^2]. \quad (6)$$

Similarly, for the ripple trough centered on the filter (spectrum  $1 - m \cos 2\pi Dg$ ), the transmitted power  $P_{\text{tr}}$  is

$$P_{\text{tr}} = E[1 - m/(1 + \pi^2 D^2 E^2/4)^2] \quad (7)$$

and the ratio of output signals at a ripple phase reversal is

$$\frac{P_{\text{peak}}}{P_{\text{tr}}} = \frac{(1 + \pi^2 D^2 E^2/4)^2 + m}{(1 + \pi^2 D^2 E^2/4)^2 - m}. \quad (8)$$

Suppose that a change in the transmitted power is detectable when this ratio exceeds a certain differential threshold  $R_{\text{thr}}$ . Substituting  $P_{\text{peak}}/P_{\text{tr}} = R_{\text{thr}}$  to Eq. (8) gives the ripple depth threshold  $m_{\text{thr}}(D)$ :

$$m_{\text{thr}}(D) = (1 + \pi^2 D^2 E^2/4)^2 (R_{\text{thr}} - 1) / (R_{\text{thr}} + 1). \quad (9)$$

Equation (9) shows that the lowest ripple-depth threshold is  $(R_{\text{thr}} - 1)/(R_{\text{thr}} + 1)$  at  $D=0$ , i.e., when the phase-reversal test reduces to a change of wideband noise level. In real experiments,  $D > 0$ , thus the ripple-depth thresholds are higher than this lowest value.

Ripple-density resolution limit  $D_{\text{lim}}$  can be found from Eq. (9) taking  $m=1$  (the highest possible value of  $m$ ). It results in

$$D_{\text{lim}} = \frac{2}{\pi E} [(R_{\text{thr}} + 1)^{1/2} (R_{\text{thr}} - 1)^{-1/2} - 1]^{1/2}. \quad (10)$$

To compare this model with experimental data, the data were normalized by presenting the ripple densities  $D$  in terms of equivalent rectangular bandwidth  $E$  according to



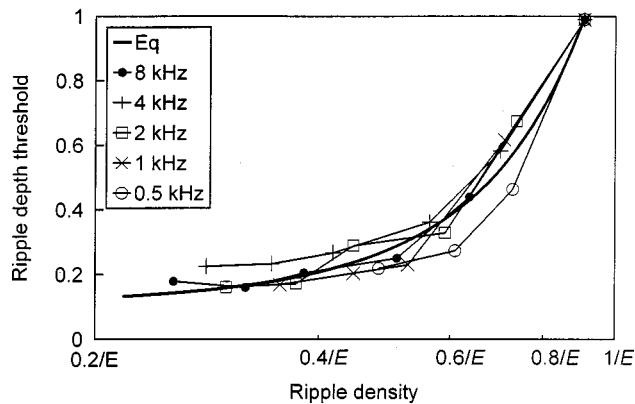


FIG. 4. Comparison of model predictions with experimental data. Eq—a function defined by Eq. (9); other curves—normalized experimental data for center frequencies from 0.5 to 8 kHz, as indicated.

Eq. (10) at a certain value of  $R_{thr}$ , and the parameter  $R_{thr}$  was adjusted to obtain the best fit of the function  $m_{thr}(D)$  to the experimental data according to the least-mean-square criterion (Fig. 4). Being normalized, all the experimental curves grouped densely (by definition, they met a common point at  $m_{thr}=1$ ). The best fit was found at  $R_{thr}=1.24$  (i.e., about 1 dB); this is close to many estimations of the differential threshold in humans (e.g., Jestead *et al.*, 1977; also review Rabinowitz *et al.*, 1976; Kay, 1982; He *et al.*, 1998). At this  $R_{thr}$  value, Eq. (9) gives the lowest ripple-depth threshold (at  $D=0$ ) of 0.11, and the ripple-depth thresholds at low but nonzero ripple densities ( $0.3/E$  to  $0.4/E$ ) of around 0.2. As for the ripple-density resolution, Eq. (10) gives a value of  $D=0.91/E$ . At found ripple-density resolution limits as high as 14.3 relative units, this results in relative  $E$  values of 0.06. This is a narrower bandwidth (better tuning) than that of peripheral auditory filters (around 0.1) found in a number of masking experiments (review Glasberg and Moore, 1990). Therefore the filter bandwidth  $E$  used in the model cannot be attributed to peripheral filters only and should be considered as an overall equivalent of all processes determining discrimination of spectral ripples. It seems that this simple model can be adopted as a first approximation of relationships between ripple depth and density resolutions.

## ACKNOWLEDGMENT

The study was supported by the Russian Foundation for Basic Research, Grant No. 96-04-48036

- Bilsen, F. A., and Wieman, J. L. (1980). "Atonal periodicity sensation for comb filtered noise signals," in *Psychophysical and Behavioral Studies in Hearing*, edited by G. van der Brink and F. A. Bilsen (Delft U. P., Delft), pp. 379–382.
- Durlach, N. I., Braida, D. L., and Ito, Y. (1986). "Towards a model for discrimination of broadband signals," *J. Acoust. Soc. Am.* **80**, 63–72.
- Glasberg, B. R., and Moore, B. C. J. (1990). "Derivation of auditory filter shapes from notched-noise data," *Hear. Res.* **47**, 103–138.
- Green, D. M. (1983). "Profile analysis: A different view of auditory intensity discrimination," *Am. Psychol.* **38**, 133–142.

- Green, D. M. (1988). *Profile Analysis: Auditory Intensity Discrimination* (Oxford U. P., New York).
- Green, D. M. (1992). "On the number of components in profile-analysis tasks," *J. Acoust. Soc. Am.* **91**, 1616–1623.
- Green, D. M., Mason, C. R., and Kidd, Jr., G. (1984). "Profile analysis: Critical band and duration," *J. Acoust. Soc. Am.* **75**, 1163–1167.
- Green, D. M., Onsan, Z. A., and Forrest, T. G. (1987). "Frequency effects in profile analysis," *J. Acoust. Soc. Am.* **81**, 692–699.
- He, N., Dubno, J. R., and Mills, J. H. (1998). "Frequency and intensity discrimination measured in a maximum-likelihood procedure from young and aged normal-hearing subjects," *J. Acoust. Soc. Am.* **103**, 553–565.
- Houtgast, T. (1974). "Masking patterns and lateral inhibition," in *Facts and Models in Hearing*, edited by E. Zwicker and E. Terhardt (Springer, Berlin), pp. 258–265.
- Houtgast, T. (1977). "Auditory-filter characteristics derived from direct-masking and pulsation-threshold data with a rippled-noise masker," *J. Acoust. Soc. Am.* **62**, 409–415.
- Jesteadt, W., Wier, C. C., and Green, D. M. (1977). "Intensity discrimination as a function of frequency and level," *J. Acoust. Soc. Am.* **61**, 169–177.
- Kay, R. H. (1982). "Hearing of modulation in sounds," *Physiol. Rev.* **62**, 894–975.
- Levitt, H. (1971). "Transformed up-down methods in psychoacoustics," *J. Acoust. Soc. Am.* **49**, 467–477.
- Patterson, R. D., Nimmo-Smith, I., Weber, D. L., and Milroy, R. (1982). "The deterioration of hearing with age: Frequency selectivity, the critical ratio, the audiogram, and speech threshold," *J. Acoust. Soc. Am.* **72**, 1788–1803.
- Patterson, R. D., Handel, S., Yost, W. A., and Datta, A. J. (1996). "The relative strength of the tone and noise components in iterated rippled noise," *J. Acoust. Soc. Am.* **100**, 3286–3294.
- Pick, G. F. (1980). "Level dependence of psychophysical frequency resolution and auditory filter shape," *J. Acoust. Soc. Am.* **68**, 1085–1095.
- Pick, G. F., Evans, E. F., and Wilson, J. P. (1977). "Frequency resolution in patients with hearing loss of cochlear origin," in *Psychophysics and Physiology of Hearing*, edited by E. F. Evans and J. P. Wilson (Academic, New York), pp. 273–282.
- Popov, V. V., and Supin, A. Ya. (1984). "Quantitative measurement of frequency resolving power of the human hearing," *Dokl. Akad. Nauk SSSR (Proc. Acad. Sci. USSR)* **278**, 1012–1016.
- Rabinowitz, W. M., Lim, J. S., Braida, L. D., and Durlach, N. I. (1976). "Intensity perception. VI. Summary of recent data on deviations from Weber's law for 1000-Hz tone pulses," *J. Acoust. Soc. Am.* **59**, 1506–1509.
- Supin, A. Ya., Popov, V. V., Milekhina, O. N., and Tarakanov, M. B. (1994). "Frequency resolving power measured by rippled noise," *Hear. Res.* **78**, 31–40.
- Supin, A. Ya., Popov, V. V., Milekhina, O. N., and Tarakanov, M. B. (1997). "Frequency-temporal resolution of hearing measured by rippled noise," *Hear. Res.* **108**, 17–27.
- Supin, A. Ya., Popov, V. V., Milekhina, O. N., and Tarakanov, M. B. (1998). "Ripple density resolution for various rippled-noise patterns," *J. Acoust. Soc. Am.* **103**, 2042–2050.
- Wilson, J. P., and Evans, E. F. (1971). "Grating acuity of the ear: psychophysical and neurophysiological measures of frequency resolving power," in *7th International Congress on Acoustics* (Akademiai Kiado, Budapest), Vol. 3, pp. 397–400.
- Yost, W. A. (1982). "The dominance region and ripple-noise pitch: A test of the peripheral weighting model," *J. Acoust. Soc. Am.* **72**, 416–425.
- Yost, W. A., and Hill, R. (1979). "Models of the pitch and pitch strength of ripple noise," *J. Acoust. Soc. Am.* **66**, 400–410.
- Yost, W. A., Hill, R., and Perez-Falcon, T. (1977). "Pitch discrimination of ripple noise," *J. Acoust. Soc. Am.* **63**, 1166–1173.
- Yost, W. A., Patterson, R. D., and Sheft, S. (1996). "A time domain description for the pitch strength of iterated rippled noise," *J. Acoust. Soc. Am.* **99**, 1066–1078.